Biointerface Research in Applied Chemistry
Platinum Open Access Journal (ISSN: 2069-5837)

Article
Volume 11, Issue 6, 2021, 14463 - 14479
https://doi.org/10.33263/BRIAC116.1446314479

Nanocurcumin Improves the Therapeutic Role of Mesenchymal Stem Cells in Liver Fibrosis Rats

Dalia D. Abd El-Monem [1], Amina A.S. Abdel Rahman [1], Shereen H.B. Elwakeel [1,*]

[1] Zoology Department, Faculty of Women for Arts, Science and Education, Ain Shams University, Asmaa Fahmy Street, Heliopolis, Cairo; dalia.demerdash@women.asu.edu.eg (D.D.A.E.-M.); amina_abdelrahman@women.asu.edu.eg (A.A.S.A.R.); sherien.elwakeel@women.asu.edu.eg (S.H.B.E.);
* Correspondence: sherien.elwakeel@women.asu.edu.eg;

Scopus Author ID 56349855600
Received: 6.02.2021; Revised: 5.03.2021; Accepted: 10.03.2021; Published: 22.03.2021

Abstract: Nano-curcumin (Nano-Cur) is a promising therapeutic agent that has a wide array of effective medicinal potentials. Therefore, the present inquiry aimed to assess Nano-Cur's impact on the therapeutic effect of bone-marrow-derived mesenchymal stem cells (BM-MSCs) in the rat model of liver fibrosis prompted by carbon tetrachloride (CCl_4). Liver fibrosis was developed in 30male Wistar albino rats which were divided into five groups, six animals each. The 1st group (CCl_4 group) was sacrificed immediately after the induction of liver fibrosis. The 2nd group received a single iv injection of BM-MSCs and left for 4weeks, the3rd group received 100mg/kg b.w. Nano-Cur 3times/week for 4weeks, the 4th group received a single iv injection of 10^7 BM-MSCs accompanied with Nano-Cur 3times/week for 4weeks, and the 5th group left for 4weeks without any intervention. Data revealed that treatment with BM-MSCs plus Nano-Cur alleviated liver fibrosis through reducing liver oxidative stress and restoring both liver histological picture and enzymatic profile. Additionally, companied treatment resulted in reducing TGFβ1 levels and attenuating the expression of Smad 2,3 and collagen I, III genes. Conversely, most of the pathological lesions were still detected in the recovery group. Nano-Cur improves the therapeutic role of BM-MSCs in liver fibrosis rats.

Keywords: liver fibrosis; nano-curcumin; mesenchymal stem cells

1. Introduction

The liver is a vital organ that performs a wide array of metabolic activities required for nutrition, homeostasis, and immune defense [1]. It is the main site for the production of plasma proteins and synthesis plus degradation of steroid hormone. Also, the liver plays an important role in the detoxification of various toxic endogenous and xenobiotic substances through different metabolic pathways, including the CYP450 enzyme [2]. These enzymes break down toxic substances and make them more polar to facilitate their removal through the kidney. Unfortunately, the detoxification process may result in the generation of different kinds of toxic reactive oxygen species (ROS) and electrophiles that cause liver injury and lead to liver malfunction [3]. Even so, the liver has great inherent regenerative potentials in response to injury [4]. But these potentials can be disturbed by diseases that cause chronic injury and lead to the onset of liver fibrosis and cirrhosis. In the liver, hepatocytes are the fundamental unit, covering about60%oftheentirenumberofcells and 80% of the liver's overall volume [5]. While, hepatic stellate cells (HSCs), also known as Ito cells, vitamin-A-storing cells, and lipocytes, account for 5%–8% of the cells and reside in the Disse space, acting as the main sites of vitamin

A storages and the main producers of extracellular matrix (ECM) proteins in the injured liver, including collagens (I, III, and IV), fibronectin and other proteins [6]. Following liver injury, quiescent HSCs activate due to ROS's stimulation, inflammatory cytokines, and apoptotic signals, and transdifferentiate into α-smooth muscle actin (SMA)-positive, myofibroblasts like cells [7]. The activated HSCs then migrate and settle at the tissue repair sites, where it secrets large quantities of ECM and regulates its degradation. In fibrotic conditions, a significant change in the amount and composition of ECM occurs along with widespread scar formation and disruption of the liver architecture [8]. The liver in the advanced stage of fibrosis has about 6 times more ECM than the normal average as the accumulation of ECM results from the unbalance between ECM synthesis and degradation [9]. Many aetiologies can induce liver fibrosis, such as alcohol abuse, viral infection, fatty liver diseases, autoimmune hepatitis, hepatic toxins, parasite Schistosoma, and cholestasis [7,10,11]. In the long run, liver fibrosis may lead to cirrhosis and ultimate death due to chronic liver failure [12].

Mesenchymal stem cells (MSCs) are multipotent stromal cells that present in almost all postnatal tissues. MSCs capable of self-renewing and can differentiate into specific cell types generating mature cells and tissues of mesodermal origin. Recently, several studies have revealed the ability of MSCs to act as therapeutic mediators in a variety of diseases, including pancreatitis [13], acute lung injury [14], rheumatoid arthritis or osteoarthritis [15], and liver diseases [16]. The therapeutic role of stem cells in treating acute and chronic liver failure is attributed to their extensive immunoregulatory properties by reducing the immune and inflammatory responses via secreting growth factors, exosomes, and many cytokines [17]. Additionally, MSCs can differentiate into hepatocytes and increase hepatocytes renewal, enhancing the liver functionally and structurally [18].

On the other hand, curcumin (Cur), the major constituent of turmeric, is a hydrophobic polyphenolic pigment derived from the herb Curcuma longa's rhizome, a member of the Zingiberaceae family [19]. For centuries, Cur has been used as a food additive, remedy, dye, and natural pigment in the cosmetic, textile, and food industries [20]. Cur possesses antibacterial, anti-inflammatory, anti-virus, and even anti-cancer properties [21]. Several bioavailability studies conducted on laboratory animals and humans have categorized the amount and rate at which Cur is absorbed, appeared in the plasma, and reached its target organs [22]. These studies revealed the low bioavailability of curcumin, which is attributable to its low intestinal absorption and rapid liver tissue metabolism. As a consequence of the poor solubility and bioavailability of Cur, its use in clinical applications is limited. Therefore, different approaches have been proposed to enhance Cur bioavailability by improving its solubility in aqueous solutions, such as forming a complex with metal ions as Zn^{+2}, Cu^{+2}, Mg^{+2}, and Se^{+2} and the formation of solid dispersion [23]. Additionally, the bioavailability of Cur can be enhanced by altering its analogs structurally, co-administration with piperine, borneol, liposomes, phospholipids, and the formation of nanoparticles [24-27].

Nanoparticles formation (1nm - 100 nm) from any conventional material changes its physical, chemical, and biological properties. The large surface area per weight of nanoparticles versus other particles makes them more reactive to other molecules, enhances their solubility, facilitates their way through animal cell membranes, and makes them rapidly interact with biological systems [28]. The use of nanoparticles has arisen as a quickly developing area for the safe delivery of several therapeutic agents in different pathological treatments, including liver ailments [29]. Nano-Curcumin (Nano-Cur) is completely soluble in aqueous media, which enhances its absorption, cellular uptake, bioavailability, and ultimate

efficiency [26]. This provides an opportunity to expand the clinical range of Nano-Cur applications. Therefore the present study was conducted to evaluate the impact of nano-curcumin (Nano-Cur) on the therapeutic role of bone-marrow-derived mesenchymal stem cells (BM-MSCs) in the rat model of liver fibrosis prompted by carbon tetrachloride (CCl4).

2. Materials and Methods

2.1. Chemicals.

Dulbecco's modified Eagle's medium (DMEM), fetal bovine serum (FBS), penicillin-streptomycin solution, and 0.25% trypsin – 1 mM EDTA solution were purchased from GIBCO/BRL. Carbon tetrachloride (CCl_4) (concentration 100%), PKH26 were purchased from Sigma Company (Saint Louis, Missouri USA), and olive oil was obtained from Algomhoria Company, Egypt

- CCl_4 solution was obtained by dissolving 100 mg of CCl_4 in 100 mL of olive oil (1:1).
- Nano-curcumin was purchased from NanoTech Egypt for Photo-Electronics, El-Wahaat Road, Dreamland city, Entrance 3, City of 6 October, Al Giza, Egypt.

2.2. Animals.

Fifty-four healthy male albino rats of Wistar strain weighing around 150 ± 20 g (9-11 weeks old)and from the same genetic and health status source were used during the experiment. The Animals were bought from the animal house of EL-Salam farm, Giza, Egypt, randomly housed in stainless steel cages, kept in an air-conditioned room with a 12 h light-dark cycle and humidity 50%–70%. Animals were permitted to adapt to laboratory conditions for about 14 days before the beginning of the experiment. Laboratory rodent diet and tap water were accessible ad libitum. Animal welfare and experimental procedures were carried out following the guidelines of the Committee on Care and Use of Experimental Animal Resources, Medical Research Center, Ain Shams University. Animals were handled gently with care during the experiment, and all efforts were made to minimize animal distress.

2.3. Experimental design.

2.3.1. Liver fibrosis (treatment groups).

30 animals were injected intraperitoneally with 0.3 mL of CCl_4 twice a week for eight weeks to induce liver fibrosis [30]. Rats have randomly distributed into 5 groups 6 animals each as follow:

Group 1 (CCl_4 group) was immediately sacrificed after 8 weeks of receiving CCl_4. Histological and biochemical examinations were done to assure that animals have liver fibrosis.

Group 2 (BM-MSCs/treatment group) were injected intravenous by a single dose10^7 of BM-MSCs suspended in 0.5 mL PBS and left for other 4 weeks.

Group 3 (Nano-Cur/treatment group) rats were orally received 100 mg/kg b.w. of Nano-Cur 3times/week for 4 weeks.

Group 4 (BM-MSCs + Nano-Cur /treatment group) animals with liver fibrosis were injected with a single i.v. dose of 10^7 BM-MSCs and received Nano-Cur by oral gavage 3 times a week for 4 weeks.

Group 5 (CCl_4/recovery group) after the induction of liver fibrosis animals in this group was left for another four weeks without any intervention.

2.3.2. Control groups.

24 animals were randomly divided into 4 groups 6 animals each as follow:

Group 6 (vehicle control): received 0.3 mL of olive oil by oral gavage twice a week for eight weeks.

Group 7 (BM-MSCs/control group) were injected intra-venous (IV) by a single dose10^7 of BM-MSCs alone and were sacrificed after four weeks.

Group 8 (Nano-Cur/control group): received 100 mg/kg b.w. of Nano-Cur by oral gavage three times a week for four weeks.

Group 9 (BM-MSCs/Nano-Cur group) were injected intra-venous (IV) by a single dose10^7 of BM-MSCs and received 100 mg/kg b.w. of Nano-Cur by oral gavage three times a week for four weeks.

Deep isoflurane inhalation was used to sacrifice animals. Blood was immediately extracted by cardiac puncture during deep anesthesia; it was slowly withdrawn to prevent the heart from collapsing, left to coagulate at room temperature for 60 min, then centrifugated at 3000 g for 30 min at 4 °C to obtain serum for biochemical analysis. Additionally, the liver was dissected out, cleaned, weighed, and prepared for further investigations.

2.4. Culture and isolation of BM-MSCs.

For isolation of BM-MSCs, male white albino rats (6 weeks old) were sacrificed by cervical dislocation. BMCs were flushed from the tibia and femur bones with DMEM complemented with 10% fetal bovine serum. BM-mononuclear cells were separated from whole BM cells with a density gradient centrifugation using Ficoll (Pharmacia). After centrifugation, mononuclear cells were placed in a 25 cm^2 Falcon flask and incubated in a complete culture medium enhanced with 1% penicillin-streptomycin at 37°C with 5% CO_2. The culture solution was changed after three days of incubation, and cells that not adhered to the flask walls were removed. Constantly, the culture solution was changed every 3 days until cells achieved 90% confluence. For cell harvesting, cultures were washed with PBS, adhered MSCs on plastic flasks were dissociated using 0.25% trypsin in 1mM EDTA for 5 min at 37°C and centrifuged. Then serum-supplemented media were added to the harvested cells in 50 cm^2 Falcon flasks and marked as passage 1 (P1). The media were changed every 3 days until the cells were developed to confluence. The procedures were repeated, and the cells were marked as passage 2 (P2) and so on till passage 4 (P4). BM-MSCs were selected based on their adherence to plastic, morphology, their power to differentiate into osteocytes and chondrocytes, and their surface marker as CD29, CD34, CD45, CD73, CD90 & CD105 by flow cytometry analysis.

2.4.1. Labeling of MSCs with PKH26.

BM-MSCs were labeled with PKH26 from Sigma Company (Saint Louis, Missouri USA).

2.5. Biochemical analysis.

2.5.1. Measurement of serum biomarkers ALT, AST, and albumin.

According to the corresponding manufacturer's instructions, Alanine aminotransferase (ALT), Aspartate aminotransferase (AST), and albumin were determined using clinical test kits.

2.5.2. Oxidative stress and antioxidant activity.

- Liver tissues were homogenized in chilled 10 mM PBS with optimal pH 7.4, centrifuged, and the supernatant was used to measure the following:
- Malondialdehyde (MDA) the final product of lipid peroxidation using the thiobarbituric acid (TBA) test [31];
- Catalase (CAT) Activity by assessing the decomposition of H_2O_2 at 240 nm[32];
- Total antioxidant activity (TAA)[33].

2.5.3. Estimation of tissue levels TGF-β1 by ELISA.

Tissue levels TGF-β1 were measured using the enzyme-linked immunosorbent assay (ELISA) method using the DRG ELISA TGF-β1 kit (My BioSource.com,USA, Catalog Number: MBS282195) according to the kit manufacturer'sinstructions.

2.6. Western Blot analysis (using V3 Western Workflow™ Complete System, Bio-Rad® Hercules, CA, USA).

Briefly, proteins were extracted from liver tissues, and 20µg of total protein/sample were separated on 10% SDS-PAGE using the Bio-Rad Mini-Protein II system. Fractioned proteins were transferred to polyvinylidene difluoride (PVDF) membranes (Pierce, Rockford, IL, USA) using the Bio-Rad Trans-Blot system according to manufacturer's instructions and blocked at room temperature for 1h with 5% (w/v) skimmed milk powder in Tris-buffered saline-Tween (TBS-T: 0.05 M Tris, 0.138 M NaCl, 0.0027 M KCl, 0.05–0.1% Tween (Sigma)). After blocking, the PVDF membranes were washed 3 times 5 min each, incubated at 4 ^{o}C overnight on a shaker with specific primary antibodies against Smad2 (1:500), Smad3 (1:500), and anti-β-actin (1:1000) as a loading control. Next, the membranes were washed with TBS-T 3 times for 5 min each. After washing, peroxidase-labeled secondary antibodies were applied, and the membranes were incubated at 37°C for 1h. The ChemiDocTM imaging system then analyzed the band intensity with Image LabTM software version 5.1 (Bio-Rad Laboratories Inc., Hercules, CA, USA). The results were presented as arbitrary units after normalization for β-actin protein expression.

2.7. Quantitative RT-PCR analysis.

Total RNA was extracted from hepatic tissue homogenate by utilizing the RNeasy purification kit (Qiagen, Valencia, CA), as stated in the manufacturer protocol. RNA extracts were spectrophotometry quantified at 260 nm and reverse transcribed using high capacity cDNA reverse transcription kit (#K1621, Fermentas, USA). According to the manufacturer's instructions, the relative abundance of mRNA was evaluated using the SYBR Green routine on an ABI prism 7500 sequence detector system (Applied Biosystems, Foster City, California, USA). PCR primers for Col I, ColII, MMP2, and β-actins (Table 1) were purchased from

Applied Biosystems. Quantitative real-time PCR was accomplished in duplicate in a 25 mL reaction volume comprising 2X SYBR Green PCR Master Mix (Applied Biosystems), 900 nmol/l of each primer, and 2–3 mL of cDNA. Results were calculated using the v1·7 Sequence Detection Software (PE Biosystems, Foster City, CA). Relative gene expressions of Col I, Col III, and MMP2 mRNA were calculated using the comparative Ct method. All values were normalized to expression levels of β-actins used as an internal standard.

Table 1. Primers used for the real-time polymerase chain reaction.

Target gene	Forward primer (5`-3`)	Reverse primer (5`-3`)
Collagen I (Col I)	TCACCTACAGCACGCTTG	GGTCTGTTTCCAGGGTTG
Collagen III (Col III)	GTGG ACTGCCTGGACCTCCA3	GGTATCAAAGGCCCAGCTGG
Metalloproteinase 2 (MMP-2)	GATGAAGTCCGGTTTTTCAAAG	GGGGTATCCGTGTAGCACCAT
β-actin (housekeeping gene)	GGTCGGTGTGAACGGATTTGG	ATGTAGGCCATGAGGTCCACC

2.8. Histopathological and histochemical examinations of liver tissue.

2.8.1. Tissue processing.

Liver tissue samples were fixed in 10% neutral buffered formalin for 72 h. Samples were processed by dehydration in serial grades of ethanol, cleared in Xylene, sample impregnation, and embedding in paraplast tissue embedding media. 4 µm thick liver tissue sections were cut by a rotatory microtome. Tissue samples processing and staining with Harris Hematoxylin and Eosin as a general tissue examination staining method were performed as outlined by Bancroft [34]. Additionally, some of these sections were stained by Masson's trichrome stain to demonstrate collagen fibers [35].

2.8.2. Immunohistochemical staining.

Immunohistochemical staining was conducted on 4 µm thick paraffin tissue sections according to the manufacturer's protocol. Deparaffinized tissue sections were treated with 3% H_2O_2 for 20 min washed and incubated for 30 min with anti-alpha smooth muscle actin Rabbit polyclonal antibody (Abcam Ab5694) (1:100). Then, washed and incubated for 20 min with a secondary antibody HRP Envision kit (DAKO). After incubations, tissue sections were washed by PBS and incubated with diaminobenzidine (DAB) for 10 min. After washing by PBS, slides were countered, stained with hematoxylin, dehydrated, and cleared, then coverslipped for microscopic examination.

2.8.3. Microscopic analysis.

Specimens were blindly examined, and 6 representative non-overlapping fields were randomly selected per tissue section of each sample to determine the area percentage of collagen fibers in Masson's trichrome stained sections and immune-expression percentages levels of alpha SMA in immune-stained sections. Data were obtained using a Full HD microscopic imaging system (Leica Microsystems GmbH, Germany) operated by Leica Application software for tissue section analysis.

2.9. Statistical methods.

Data were represented as mean ± standard error of the mean (SEM). The differences between groups were compared using one-way analysis of variance (ANOVA) followed by

Tukey's multiple comparison test. All analysis was done using IPM-SPSS version 20. P-values less than 0.05 were considered statistically significant.

3. Results and Discussion

MSCs therapy has been proven to be an effective alternative treatment for hepatic diseases by enhancing the liver structurally and functionally. MSCs can differentiate into hepatocytes, reduce inflammatory responses, decrease apoptosis in hepatocytes, and increase regeneration [18]. The current study was conducted to evaluate the impact of nano-curcumin (Nano-Cur) on the therapeutic effect of BM-MSCs in the rat model of liver fibrosis prompted by CCl_4.

3.1. Establishment of CCl4-induced hepatic fibrosis rat model.

The rats administrated CCl_4 for eight weeks exhibited a significant decrease ($P<0.5$) in the body weight and the ratio of liver/body weight compared to the vehicle group (Figure 1), this results in harmony with Dong *et al.* [36]. CCl_4administration exhibited a significant increase ($p<0.05$) in serum AST, ALT, and albumin as compared to all control groups (Table 2). Similar results were previously reported [37]. This increase may be due to the release of these enzymes from the cytoplasm. They localized into the blood rapidly following cellular damage and reflect the degrees of liver cell membrane damage [38]. Additionally, CCl_4 administration resulted in oxidative damage to the liver tissues as demonstrated by the elevated levels of MDA, the lipid peroxidation marker, and TAA accompanied by a significant reduction ($p<0.05$) in CAT enzyme as compared to all control groups (Table 2). This may be owed to the direct effect of CCl_4 in hepatocytes by impairing plasma, lysosomal and mitochondrial membrane permeability [39]. Additionally, cytochrome P4502E1 (CYP2E1) plays a critical role in CCl_4 toxic effects in hepatocytes through metabolizing CCl_4 to reactive trichloromethyl (CCL_3*) and trichloromethyl peroxyl (CCL_3O_2*) radicals. Such radicals bind to DNA, lipids, proteins, and carbohydrates, and resulting in lipid peroxidation [40]. Furthermore, oxidative stress boosts the formation of inflammatory cytokines [41], leading to hepatocytes necrosis and inflammation, and promotes the progress of hepatic fibrogenesis [42]. Moreover, animals of the CCl_4 group showed a significant increase ($p<0.05$) in the level of TGF-β1, the key mediator of fibrogenesis (Table 2). The release of TGF-β1 by necrotic hepatocytes triggers adjacent quiescent HSCs to transdifferentiate into myofibroblasts [43]. CCl_4 administration also induced a significant increase ($p<0.05$) in smad 2 and smad 3 as compared to all control groups (Figure 2). Smads are transductive intracellular signal molecules of the TGF-β family; stimulation of TGF-β causes the phosphorylation of smads 2 and 3 that binds to smad 4 and passes into the nucleus [44]. Such signals promote the expression of the ECM genes and resulting in the synthesis of ECM proteins such as Col I and Col III [45]. Both Col I and Col III displayed a significant increase ($p<0.05$) in CCl_4 treated group (Figure 3). The accumulation of ECM proteins is a common phenomenon in liver fibrosis [46].

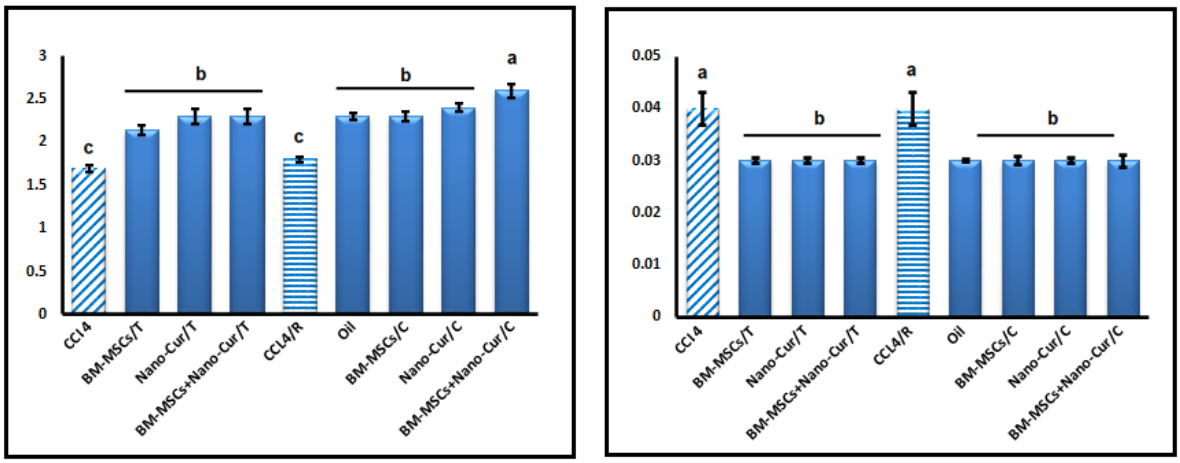

(**a**) (**b**)

Figure 1. The change in body weight (**a**) and liver/body weight ratio (**b**) after therapy with Nano-Cur and/or BM-MSCs. All values are presented as mean ± SEM (n=6). Columns that carry different letters are statistically significant (P<0.5).

Table 2. Effect of BM-MSCs and/or Nano-Cur on the mean values of the liver enzymatic profile, oxidative stress markers, and TGF-β1.

Parameters / Treatment groups	ALT	AST	Albumin	MDA (U mol/g)	TAA (mmol/g)	CAT (mmol/g)	TGF-β1
CCl_4	39.36±1.17^{a}	47.05±0.17^{a}	3.06±0.10^{b}	534.1±6.8^{a}	30.02±0.9^{a}	74.6±1.37^{e}	157 ±1.6^{a}
BM-MSCs/T	19.36±1.11^{c}	25.2±0.14^{c}	4.72±0.14^{a}	223.3±11.9^{c}	9.31±0.6^{c}	107.4±2.1^{d}	82.12±1.2^{c}
Nano-Cur/T	20.98 ±1.43^{c}	27.6 ±0.56^{c}	4.28 ±0.09^{a}	124.91±5.5^{d}	10.03±0.63^{c}	110.3±2.9^{cd}	78.88±1.12^{c}
BM-MSCs+Nano-Cur/T	15.01±1.23^{c}	24.25±0.24^{c}	4.70±0.24^{a}	157.21±8.9^{d}	9.92±0.47^{c}	124.5±2.4^{b}	60.87±1.6^{d}
CCl_4/R	27.73±1.56^{b}	32.35±0.80^{b}	3.39±0.14^{b}	458.9±9.8^{b}	26.5±0.43^{b}	79.9±1.1^{e}	130.70±1.7^{b}
Oil	13.68±1.73^{d}	17.13±1.79^{d}	4.81±0.20^{a}	156.7±8.2^{d}	11.8±0.5^{c}	106.5±2.4^{d}	36.86±1.6^{e}
BM-MSCs/C	12.98±1.38^{d}	17.18±1.8^{d}	5.31±0.14^{a}	135.8±13.4^{d}	11.14±0.6^{c}	127.6±0.8^{ab}	29.48±1.7^{e}
Nano-Cur/C	13.75±0.94^{d}	17.25±0.25^{d}	5.13±0.08^{a}	146.6±7.5^{d}	11.7±0.6^{c}	121.1±4.4^{bc}	39.00±1.7^{e}
BM-MSCs+Nano-Cur/C	12.33±1.40^{d}	19.86±0.50^{d}	4.63±0.24^{a}	120.0±6.5^{d}	11.4±0.76^{c}	136.2±2.5^{a}	37.73±1.7^{e}

All the values are presented as the mean ±SEM (n=6). Columns that carry different superscript is statistically significant (P<0.05).

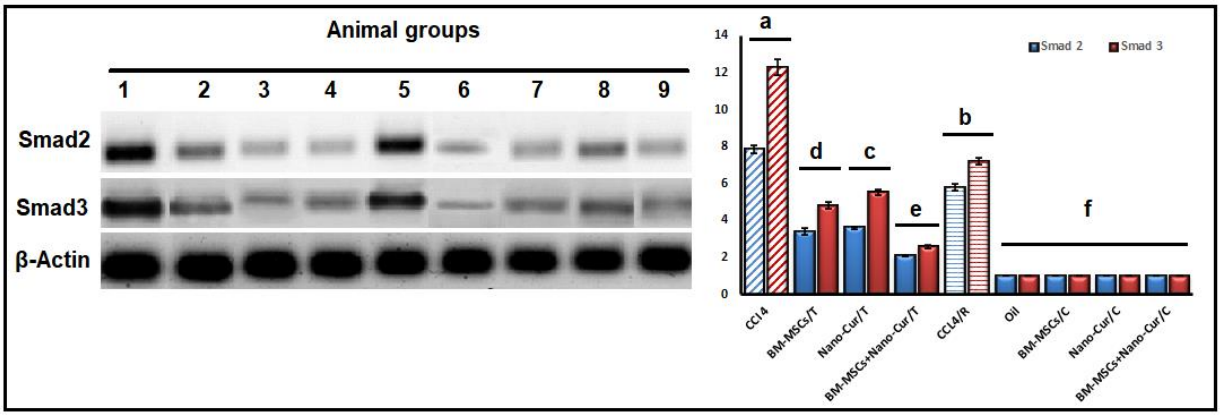

Figure 2. Effects of BM-MSCs and /or Nano-Cur on the expression of smads 2 and 3 in liver tissues. Data are expressed as mean ± SEM, (n=6). Columns that carry different letters are statistically significant (P<0.5).

1: CCl_4 group 2: BM-MSCs/T group 3: Nano-Cur/T group 4: BM-MSCs + Nano-Cur/T group
5: CCl_4 recovery group 6: oil group (vehicle) 7: BM-MSCs/C group 8: Nano-Cur/C group
9: BM-MSCs + Nano-Cur/C group

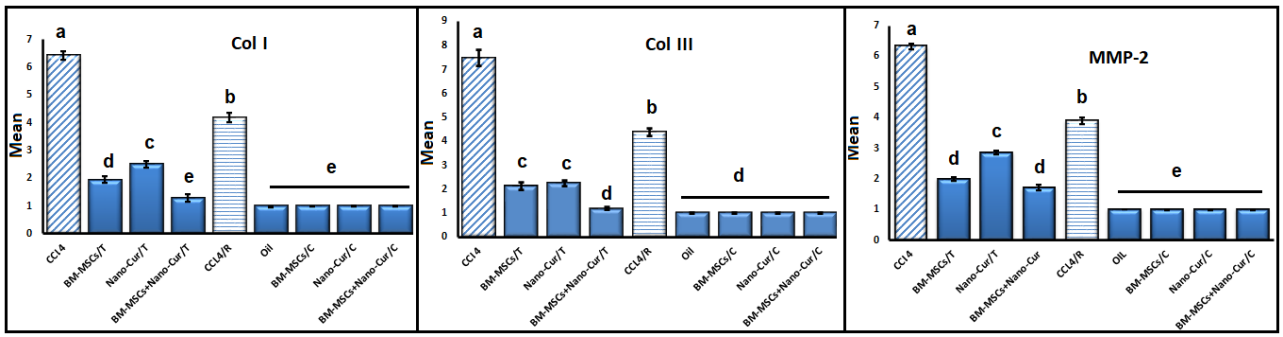

Figure 3. Col I, Col III, and MMP-2 gene expression levels after Nano-Cur and/or BM-MSCs therapy. All the values are presented as the mean±SEM (n=6). Columns that carry different letters are statistically significant (P<0.5).

The histopathological findings supported the previous results as the examination of H&E stained livers sections of the CCl_4 group (Figure 4 (1)) revealed disruption of tissue architecture, perivascular and periportal aggregations of inflammatory cells with massive neutrophilic and lymphocytic infiltration (black arrow) accompanied with large fibrous septa formation as well as bridging of fibroblasts-like hepatic stellate cells (HSCs) (black star), pseudo-lobulation was also detected. Many hepatocytes showed degenerative changes and nuclear pyknosis (yellow arrow). Such findings may be linked to the overproduction of free radicals that lead to membrane lipid peroxidation and eventually result in cellular apoptosis and necrosis and the proliferation of connective tissue and impaired hepatic structure function [47]. In contrast, all control groups showed nearly normal hepatic architecture with a central vein surrounded by normal branching and anastomosing cords with normal hepatic sinusoids in between lined by flat endothelial cells (Figure 4(6-9)).

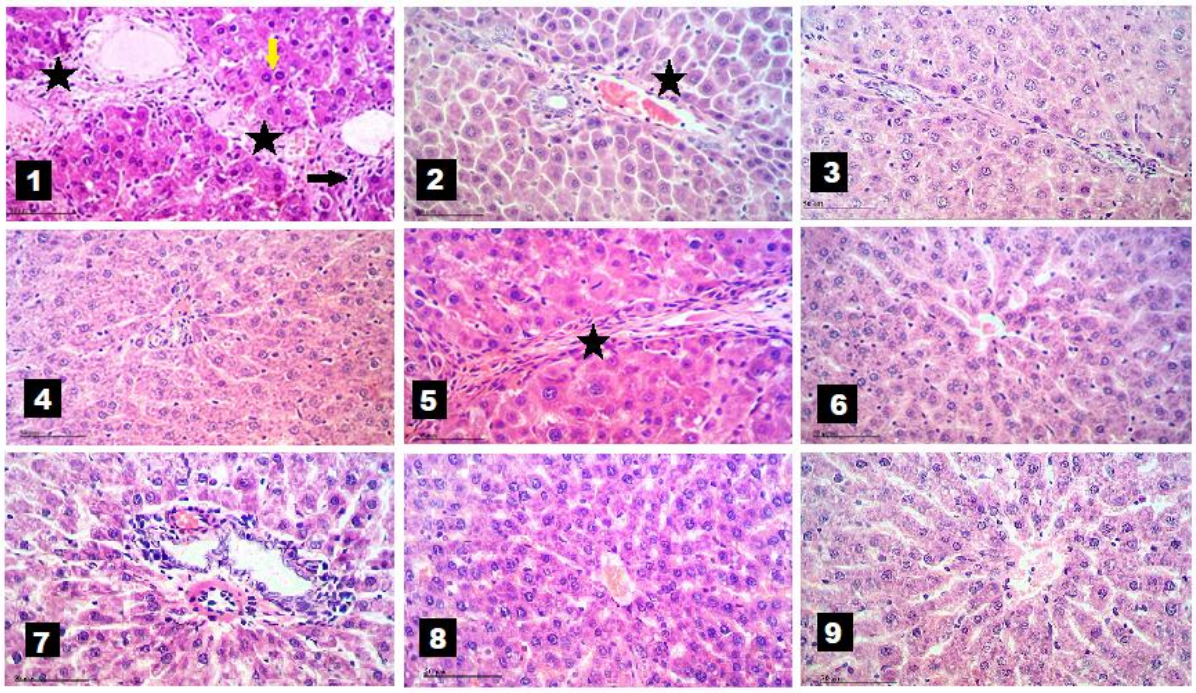

Figure 4. Photomicrographs of liver sections stained with Hematoxylin & Eosin (H&E) showing: (**1**) Disorganized hepatocytes and nuclear pyknosis (yellow arrow), aggregation of inflammatory cells (black arrow), bridging of fibroblasts-like hepatic stellate cells (black star) (CCl_4 group); (**2**) Very thin bridges of fibroblasts (BM-MSCs/T group); (**3**) Few degenerative hepatocytes with less periportal fibrosis with thin bridging fibroblasts (Nano-Cur/T group); (**4**) Few scattered degenerated hepatocytes, with less fibrosis (BM-MSCs + Nano-Cur /T group); (**5**) Degenerative hepatocytes, bridging fibroblast, (CCl_4/R group); (**6**) Oil group; (**7**) BM-MSCs/C group; (**8**) Nano-Cur/C group; (**9**) BM-MSCs+Nano-Cur/C group. (H & E x400).

Furthermore, Masson's trichrome staining displayed that most of the fibrous septa in the CCl_4 group were broad, with loosely aggregated collagen fibers around the central veins, in between hepatocyte cords, and in portal areas (yellow star) (Figure 5 (1)). The percentage of deposited collagen fibers showed a highly significant ($P<0.05$) increase in the CCl_4 group (17.75±0.73) compared to (0.52±0.09) in the vehicle group. This may be deduced by the ability of CCl_4 to increase the number of myofibroblasts as the metabolism of CCl_4 in the liver stimulates lipid peroxidation and free radicals formations, which induces inflammation and promotes progression of hepatic fibrogenesis [36]. Conversely, all control groups showed statistically non-significant differences ($P>0.05$) in the mean area percentage of collagen fibers where parenchyma of the liver in control groups appeared to be supported with stroma of a very delicate network of collagenous fibers surrounding the central veins and portal areas (Figure 5(6-9)). The immune-staining of α-SMA was performed to spot and quantify HSCs' activity (Figure 6). There was a significant increase in the area percentage of α-SMA positive cells around the fibrous septa, which are the characteristic of advanced fibrosis with the positive brownish cytoplasmic reaction in both CCl_4 and recovery groups (Figure 5(1,5)) versus all control groups (Figure 5 (6-9)).

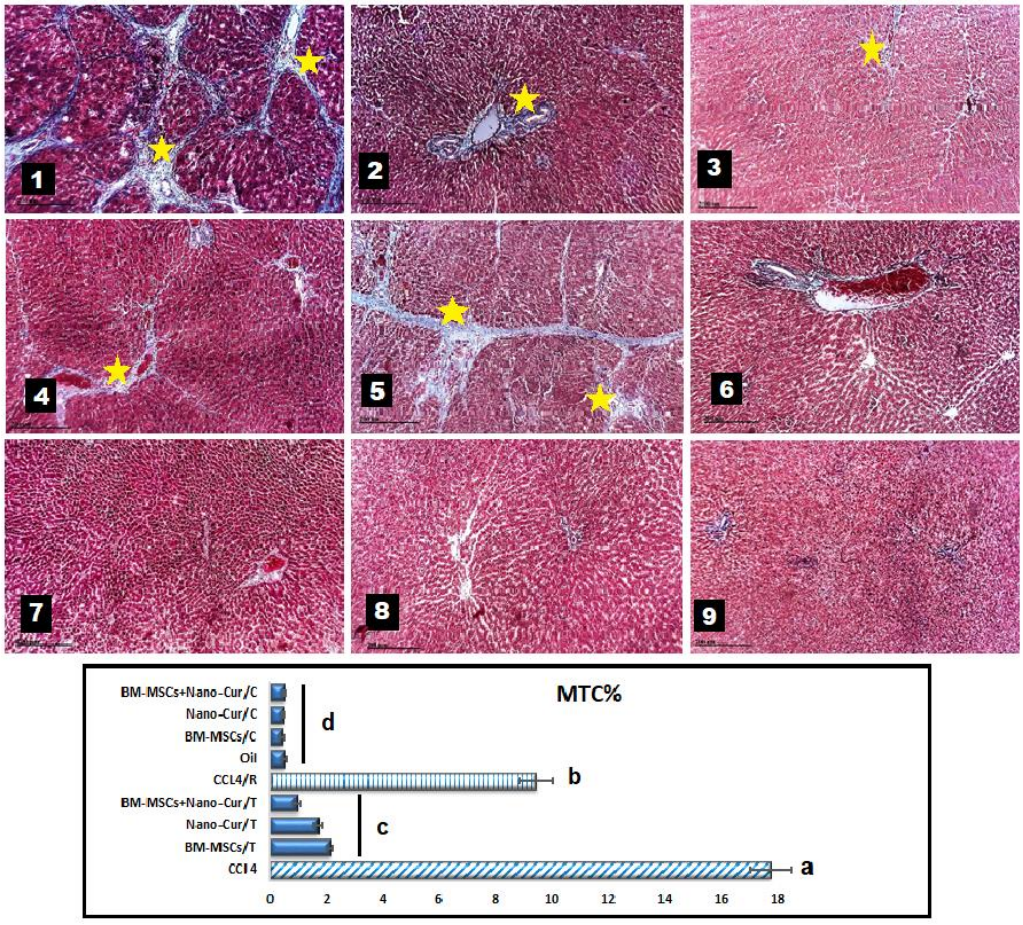

Figure 5. Liver sections stained with Masson's trichrome (**1**) broad fibrous septae of dense collagen fibers (yellow star) (CCl_4 group); (**2**) Thin fibrous septae(BM-MSCs/T group); (**3**) Few collagen fibers (Nano-Cur/T group); (**4**) (BM-MSCs + Nano-Cur /T group); (**5**) More fibrous septae of collagen fibers (CCl_4/R group); (**6**) Less collagen fibers (oil group); (**7**) BM-MSCs/C group; (**8**) Nano-Cur/C group; (**9**) BM-MSCs+Nano-Cur/C group. Data are expressed as mean ± SEM, n=6.Columns that carry different letters are statistically significant ($P<0.5$).

This reflects the deposition of extracellular matrix (ECM) proteins mediated by activated hepatic stellate cells (HSCs). HSCs undergo a phenotypic switch from quiescent, vitamin A-storing

cells to proliferative α-smooth muscle actin (SMA)-positive, myofibroblast-like cells capable of increasing collagen synthesis as a part of the liver's healing mechanism [18].

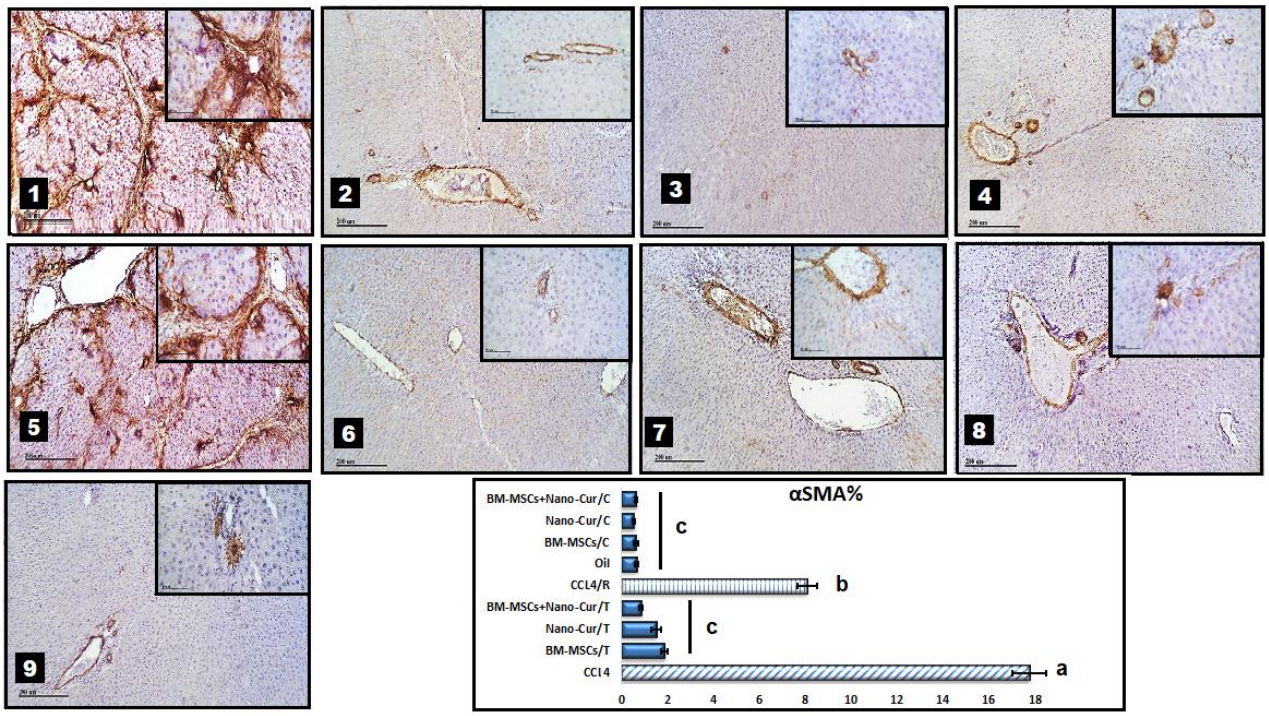

Figure 6. Photomicrographs of liver sections immune-stained with α-SMA showing: (**1**) apparent and numerous α-SMA positive cells (CCl_4 group); (**2**) few α-SMA positive cells (BM-MSCs/T group); (**3**) few numbers of α-SMA positive cells (Nano-Cur/T group); (**4**) less α-SMA positive cells (BM-MSCs + Nano-Cur /T group); (**5**) numerous α-SMA positive cells (CCl_4/R group); (**6**) few α-SMA positive cells (oil group x100); (**7**) a small number of α-SMA positive cells (BM-MSCs/C group); (**8**) Nano-Cur/C group; (**9**) BM-MSCs+Nano-Cur/C group. (100, inset x 400). Data are expressed as mean ± SEM, n=6. Columns that carry different letters are statistically significant (P<0.5).

3.2. Effect of BM-MSCs on the CCl4-induced hepatic fibrosis rat.

The analysis of MSCs Based on cell surface marker expression was positive with CD29, CD73, CD90 & CD105 and negative with CD34, CD45 (Figure7). Also, liver sections from stem cell therapy in group 2 (BM-MSCs/T) and group 4 (BM-MSCs plus Nano-Cur/T) were examined using the fluorescence microscope, the homing of the PKH26 labeled stem cells in the liver tissue were displayed in Figure 8. Results of the present investigation showed that BM-MSCs had overcome CCl_4-induced oxidative stress significantly ($p<0.05$), improving the liver enzymatic profile and decreasing MDA and TAA levels along with increasing CAT enzyme level in contrast to the CCl_4 group (Table 2). Similar results were previously reported [48]. The present results agree with Alzahrani *et al.* (2018), who confirmed the capability of MSCs-exosomes to induce a significant increase in serum antioxidant enzyme levels accompanied by a significant decrease in the lipid peroxidation level [49]. The up-regulation of ROS in CCl_4-treated liver cells owing to the antioxidant activities and hepatoprotective effects of MSCs. Cho *et al.* (2012) declared that MSCs exhibit cytoprotective effects by provoking antioxidant response elements (AREs) in CCl_4-induced liver injury [40]. Moreover, BM-MSCs treated group showed a significant ($p<0.05$) suppression in the overexpression of collagen type I and III (Figure 3) and TGF-β1 (Table 2), accompanied by upregulation of MMP2 (Figure 3) compared to CCl_4 treated group. Previous evidence has shown that MSCs can produce antifibrotic growth factors and cytokines, which play a vital role in attenuating

fibrosis through down-regulating the expression of TGF-β1 [50] and promoting ECM restoring by down-regulating the expression of collagens and up-regulating the expression of MMPs [51]. The present results displayed that BM-MSCs have significantly reduced ($p<0.05$) smad 2 and smad 3, which suggests that the inhibitory effect of BM-MSCs on CCl_4-induced fibrosis is due to its effect on TGFβ/SMAD signalling pathways [14].

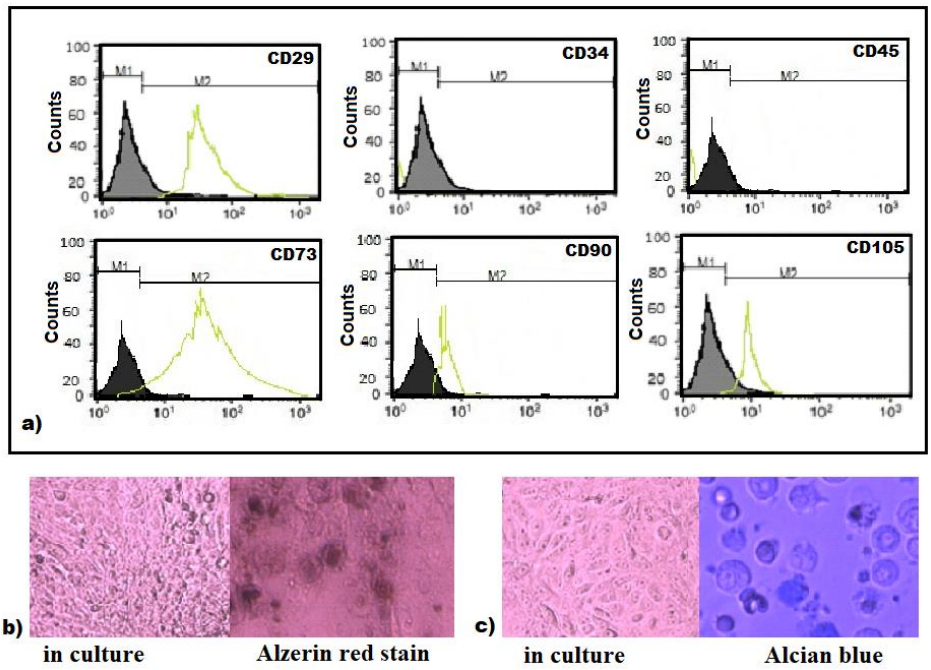

Figure7. Characteristics of BM-MSCs. (**a**) MSCs were positive for CD29, CD73, CD90, and CD105 but negative for CD34 and CD45, (**b-c**) show the capability of MSCs to differentiate towards (**b**) osteoblasts and (**c**) chondrocytes.

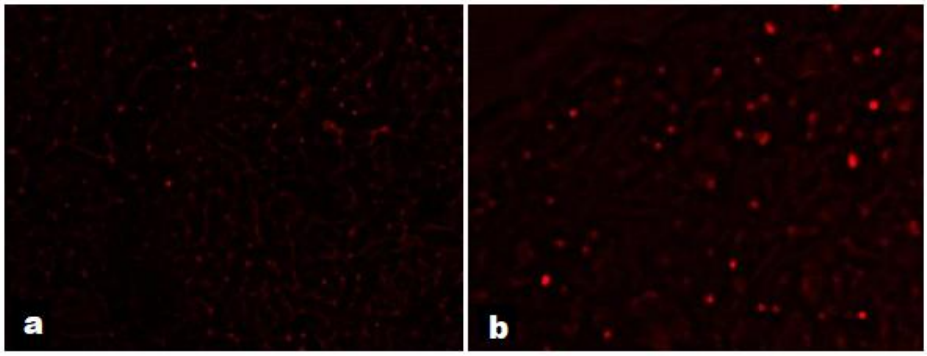

Figure8. Detection of MSCs labeled with PKH26 fluorescent dye in liver tissue after injection with (**a**) BM-MSCs alone and (**b**)BM-MSCs plus Nano-Cur. MSCs labeled with PKH26 showed strong red autofluorescence after transplantation into rats, confirming that these cells were seeded into the liver tissue.

Furthermore, the light microscopic examination of the BM-MSCs treated group displayed enhancement in hepatic tissue architecture, a result similar to that of Alzahrani *et al.* [49] and Aithal *et al.* [52]. Where most of the hepatocytes in BM-MSCs treated, the group appeared nearly as normal as those in control groups (Figure 4 (2)). Both the area percentages of the collagen fibers and the α -SMA positive cells were significantly decreased ($p<0.05$) as compared to the CCl_4 group. This may be due to the immunomodulatory characteristic of MSCs that suppress chronic inflammation and attenuate fibrosis in the liver by modulating proliferation and apoptosis of HSCs, secretion of pro-fibrotic TGF-β, and by regulating deposition of collagen [53], as MSCs permanently remain in the injured livers and can differentiate into myofibroblasts rather than in hepatocytes [54]. These results are supported

by Chen *et al.* (2011), who directly co-cultured MSCs with HSCs and revealed significant suppression in the proliferation and α-SMA expression of HSCs through cell-cell contact, and this activity is partially mediated by Notch pathway activation [55].

3.3. Effect of Nano-Cur and /or BM-MSCs plus Nano-Cur on the CCl4-induced hepatic fibrosis rat.

Curcumin is known to have a broad range of therapeutic and pharmacological properties. Over a while, considerable attention has been paid to improve the bioavailability of native Cur, but lately, nano therapy has significantly enhanced its therapeutic efficacy. Cur nanoparticles' encapsulation enhances its chemical stability and avoids its enzymatic and pH degradation [56], and increases its circulation inside the body [57]. The results of this study revealed that the administration of Nano-Cur alone or plus BM-MSCs significantly attenuated the progression of hepatic fibrosis induced by CCl_4 in rat models. Nano-Cur alone or plus BM-MSCs significantly reduced liver enzyme levels and lipid peroxidation. The decrease in the Nano-Cur treated groups' liver enzymes is due to the potent antioxidant activity of Cur [58]. Cur as a strong cytochrome p450 inhibitor can stabilize antioxidant enzymes and non-enzymatic antioxidants [59]. Cur also increases the levels of the antioxidant enzymes. Cur was found to prompt reduced glutathione synthesis, resulting in a noticeable reduction in the lipid peroxidation products such as lipid hydroperoxide and MDA [60]. In the present study, Nano-Cur significantly decreased the severity of liver necro-inflammation, significantly repressed HSCs activation, decreased the accumulation of collagen, and increased matrix metalloproteinases 2 (MMP2). These results agree with the result of Kang *et al.* [61]. These changes were accompanied by downregulation of TGF-β1 and smad 2,3 expression in the livers of rats with hepatic fibrosis. Our results in harmony with Rahmaniah *et al.* (2017), who concluded that Nano-Cur significantly decreased HSCs proliferation by decreasing TGF-β protein levels[62]. MMPs are the major enzymes involved in ECM degradation and are linked to numbers of acute and chronic liver disorders [63]. As well, HSCs play a significant role in collagen deposition [64]. Supriono *et al.* (2018) declared that the inhibitory effect of Cur on MMP-2 expression enhances HSC apoptosis, inhibiting fibrogenesis[65].

Moreover, treatment by Nano-Cur alone or plus BM-MSCs revealed remarkable improvement in the histological appearance of the liver architecture (Figure 4(3,4)). Animals treated with Nano-Cur alone (Figure 5 (3)) or plus BM-MSCs (Figure 5 (4)) exhibited less thin bridging fibroblasts supported by a decrease in the mean area percentages of both collagen fibers (Figure 5) & α-SMA (Figure 6). The remarkable enhancement in almost all examined parameters after treatment with Nano-cur plus BM-MSCs compared to treatment with BM-MSCs alone and Nano-Cur alone may be owed to the good regulatory effect of Cur on BMSCs [66]. Cur and Nano-Cur increased the survival rate of human-derived MSCs [67]. It was reported that Cur could protect BM-MSCs from injuriousness and aging and invigorate its proliferation and differentiation[68].

4. Conclusions

The present study demonstrated that Nano-Cur has a synergistic effect on stem cell therapy. The present results displayed a remarkable improvement in the liver function and structure when rats were treated with both Nano-Cur and BM-MSCs together compared to

Nano-Cur and stem cells separately. These results suggest that sync treatment of Nano-Cur and stem cells could be a promising approach to treating liver-injured tissues.

Funding

This research received no external funding.

Acknowledgments

This research has no acknowledgment.

Conflicts of Interest

The authors declare no conflict of interest.

References

1. Gu, X.; Manautou, J.E. Molecular mechanisms underlying chemical liver injury. *Expert Rev. Mol. Med.* **2012**, *14*, e4, https://doi.org/10.1017/S1462399411002110.
2. Peter Guengerich, F.; Avadhani, N.G. Roles of Cytochrome P450 in Metabolism of Ethanol and Carcinogens. In Proceedings of Alcohol and Cancer, Cham, 2018; 15-35,https://doi.org/10.1007/978-3-319-98788-0_2.
3. Brewer, C.T.; Chen, T. Hepatotoxicity of Herbal Supplements Mediated by Modulation of Cytochrome P450. *Int. J. Mol. Sci.* **2017**, *18*,https://doi.org/10.3390/ijms18112353.
4. Kung, J.W.C.; Forbes, S.J. Stem cells and liver repair. *Curr. Opin. Biotechnol.* **2009**, *20*, 568-574,https://doi.org/10.1016/j.copbio.2009.09.004.
5. Vekemans, K.; Braet, F. Structural and functional aspects of the liver and liver sinusoidal cells in relation to colon carcinoma metastasis. *World Journal of Gastroenterology: WJG* **2005**, *11*, 5095,https://doi.org/10.3748/wjg.v11.i33.5095.
6. Yin, C.; Evason, K.J.; Asahina, K.; Stainier, D.Y.R. Hepatic stellate cells in liver development, regeneration, and cancer. *The Journal of Clinical Investigation* **2013**, *123*, 1902-1910, https://doi.org/10.1172/JCI66369.
7. Friedman, S.L. Mechanisms of hepatic fibrogenesis. *Gastroenterology* **2008**, *134*, 1655-1669, https://doi.org/10.1053/j.gastro.2008.03.003.
8. Cox, T.R.; Erler, J.T. Remodeling and homeostasis of the extracellular matrix: implications for fibrotic diseases and cancer. *Disease Models & Mechanisms* **2011**, *4*, 165, https://doi.org/10.1242/dmm.004077.
9. Vinken, M. Gap junctions and non-neoplastic liver disease. *J. Hepatol.* **2012**, *57*, 655-662,https://doi.org/10.1016/j.jhep.2012.02.036.
10. Anthony, B.; Allen, J.T.; Li, Y.S.; McManus, D.P. Hepatic stellate cells and parasite-induced liver fibrosis. *Parasites & Vectors* **2010**, *3*, 60, https://doi.org/10.1186/1756-3305-3-60.
11. Menessy, A.N.; Ahmed, N.A.; Abdallah, N.I.; Arif, S.S. Noninvasive predictors of hepatic fibrosis in patients with chronic hepatitis C virus in comparison with liver biopsy. *Benha Medical Journal* **2018**, *35*, 282, https://doi.org/10.5812/hepatmon.6718.
12. Heidelbaugh, J.J.; Bruderly, M. Cirrhosis and chronic liver failure: part I. Diagnosis and evaluation. *Am. Fam. Physician* **2006**, *74*, 756-762.
13. Song, G.; Ma, Z.; Liu, D.; Qian, D.; Zhou, J.; Meng, H.; Zhou, B.; Song, Z. Bone marrow-derived mesenchymal stem cells attenuate severe acute pancreatitis via regulation of microRNA-9 to inhibit necroptosis in rats. *Life Sci.* **2019**, *223*, 9-21,https://doi.org/10.1016/j.lfs.2019.03.019.
14. Zhang, L.; Li, Q.; Liu, W.; Liu, Z.; Shen, H.; Zhao, M. Mesenchymal stem cells alleviate acute lung injury and inflammatory responses induced by paraquat poisoning. *Medical science monitor: international medical journal of experimental and clinical research* **2019**, *25*, 2623,https://doi.org/10.12659/MSM.915804.
15. Serakinci, N.; Savtekin, G. Modeling mesenchymal stem cells in TMJ rheumatoid arthritis and osteoarthritis therapy. *Critical Reviews™ in Eukaryotic Gene Expression* **2017**, *27*,https://doi.org/10.1615/CritRevEukaryotGeneExpr.2017019380.

16. Gazdic, M.; Arsenijevic, A.; Markovic, B.S.; Volarevic, A.; Dimova, I.; Djonov, V.; Arsenijevic, N.; Stojkovic, M.; Volarevic, V. Mesenchymal stem cell-dependent modulation of liver diseases. *Int. J. Biol. Sci.* **2017**, *13*, 1109, https://doi.org/10.7150/ijbs.20240.
17. Volarevic, V.; Nurkovic, J.; Arsenijevic, N.; Stojkovic, M. Concise Review: Therapeutic Potential of Mesenchymal Stem Cells for the Treatment of Acute Liver Failure and Cirrhosis. *Stem Cells* **2014**, *32*, 2818-2823, https://doi.org/10.1002/stem.1818.
18. Eom, Y.W.; Shim, K.Y.; Baik, S.K. Mesenchymal stem cell therapy for liver fibrosis. *The Korean journal of internal medicine* **2015**, *30*, 580, https://doi.org/10.3904/kjim.2015.30.5.580.
19. Esatbeyoglu, T.; Huebbe, P.; Ernst, I.M.A.; Chin, D.; Wagner, A.E.; Rimbach, G. Curcumin—From Molecule to Biological Function. *Angew. Chem. Int. Ed.* **2012**, *51*, 5308-5332, https://doi.org/10.1002/anie.201107724.
20. Aggarwal, B.B.; Sundaram, C.; Malani, N.; Ichikawa, H. CURCUMIN: THE INDIAN SOLID GOLD. In *The Molecular Targets and Therapeutic Uses of Curcumin in Health and Disease*, Aggarwal, B.B., Surh, Y.-J., Shishodia, S., Eds. Springer US: Boston, MA, **2007**,1-75, https://doi.org/10.1007/978-0-387-46401-5_1.
21. Tomeh, M.A.; Hadianamrei, R.; Zhao, X. A Review of Curcumin and Its Derivatives as Anticancer Agents. *Int. J. Mol. Sci.* **2019**, *20*,https://doi.org/10.3390/ijms20051033.
22. Liu, W.; Zhai, Y.; Heng, X.; Che, F.Y.; Chen, W.; Sun, D.; Zhai, G. Oral bioavailability of curcumin: problems and advancements. *J. Drug Targeting* **2016**, *24*, 694-702, https://doi.org/10.3109/1061186X.2016.1157883.
23. Seo, S.-W.; Han, H.-K.; Chun, M.-K.; Choi, H.-K. Preparation and pharmacokinetic evaluation of curcumin solid dispersion using Solutol® HS15 as a carrier. *Int. J. Pharm.* **2012**, *424*, 18-25, https://doi.org/10.1016/j.ijpharm.2011.12.051.
24. Angélica, A.O.-F.; Josafat, A.H.-B.; Adriana, C.-G.; Ida, S.-R.; Maria Guadalupe, S.-O.; Eduardo, J.V.-C.; Hugo, S.G. Enhanced Bioavailability of Curcumin Nanoemulsions Stabilized with Phosphatidylcholine Modified with Medium Chain Fatty Acids. *Curr. Drug Del.* **2017**, *14*, 377-385,https://doi.org/10.2174/1567201813666160919142811.
25. Peng, S.; Zou, L.; Liu, W.; Li, Z.; Liu, W.; Hu, X.; Chen, X.; Liu, C. Hybrid liposomes composed of amphiphilic chitosan and phospholipid: Preparation, stability and bioavailability as a carrier for curcumin. *Carbohydr. Polym.* **2017**, *156*, 322-332, https://doi.org/10.1016/j.carbpol.2016.09.060.
26. Ipar, V.S.; Dsouza, A.; Devarajan, P.V. Enhancing Curcumin Oral Bioavailability Through Nanoformulations. *Eur. J. Drug Metab. Pharmacokinet.* **2019**, *44*, 459-480, https://doi.org/10.1007/s13318-019-00545-z.
27. Gao, Y.; Chen, G.; Luan, X.; Zou, M.; Piao, H.; Cheng, G. Improved Oral Absorption of Poorly Soluble Curcumin via the Concomitant Use of Borneol. *AAPS PharmSciTech* **2019**, *20*, 150, https://doi.org/10.1208/s12249-019-1364-5.
28. Aggarwal, P.; Hall, J.B.; McLeland, C.B.; Dobrovolskaia, M.A.; McNeil, S.E. Nanoparticle interaction with plasma proteins as it relates to particle biodistribution, biocompatibility and therapeutic efficacy. *Adv. Drug Del. Rev.* **2009**, *61*, 428-437,https://doi.org/10.1016/j.addr.2009.03.009.
29. Giannitrapani, L.; Soresi, M.; Bondì, M.L.; Montalto, G.; Cervello, M. Nanotechnology applications for the therapy of liver fibrosis. *World Journal of Gastroenterology: WJG* **2014**, *20*, 7242, https://doi.org/10.3748/wjg.v20.i23.7242.
30. Iredale, J.P.; Benyon, R.C.; Pickering, J.; McCullen, M.; Northrop, M.; Pawley, S.; Hovell, C.; Arthur, M.J. Mechanisms of spontaneous resolution of rat liver fibrosis. Hepatic stellate cell apoptosis and reduced hepatic expression of metalloproteinase inhibitors. *The Journal of Clinical Investigation* **1998**, *102*, 538-549,https://doi.org/10.1172/JCI1018.
31. Ohkawa, H.; Ohishi, N.; Yagi, K. Assay for lipid peroxides in animal tissues by thiobarbituric acid reaction. *Anal. Biochem.* **1979**, *95*, 351-358,https://doi.org/10.1016/0003-2697(79)90738-3.
32. York, S. Aebi H. Catalase. In: Methods of enzymatic analysis, Bergmeyer HU (editor), Academic press, New York, **1974**, 671-684.
33. Koracevic, D.; Koracevic, G.; Djordjevic, V.; Andrejevic, S.; Cosic, V. Method for the measurement of antioxidant activity in human fluids. *J. Clin. Pathol.* **2001**, *54*, 356-361,https://doi.org/10.1136/jcp.54.5.356.
34. Bancroft, J.; Gamble, M. A.Theory and practice of histological techniques 6th ed.; Churchil Livingstone: New York, London **2007**; 165-175.
35. Sheehan, D.C.; Hrapchak, B.B. *Theory and practice of histotechnology*; Mosby: **1980**.

36. Dong, S.; Chen, Q.-L.; Song, Y.-N.; Sun, Y.; Wei, B.; Li, X.-Y.; Hu, Y.-Y.; Liu, P.; Su, S.-B. Mechanisms of CCl4-induced liver fibrosis with combined transcriptomic and proteomic analysis. *The Journal of Toxicological Sciences* **2016**, *41*, 561-572,https://doi.org/10.2131/jts.41.561.
37. Foaud, M.A.; Kamel, A.H.; Abd El-Monem, D.D. The protective effect of N-acetyl cysteine against carbon tetrachloride toxicity in rats. *The Journal of Basic and Applied Zoology* **2018**, *79*, 14, https://doi.org/10.1186/s41936-018-0022-x.
38. Kepekçi, R.A.; Polat, S.; Çelik, A.; Bayat, N.; Saygideger, S.D. Protective effect of Spirulina platensis enriched in phenolic compounds against hepatotoxicity induced by CCl4. *Food Chem.* **2013**, *141*, 1972-1979,https://doi.org/10.1016/j.foodchem.2013.04.107.
39. Knockaert, L.; Berson, A.; Ribault, C.; Prost, P.-E.; Fautrel, A.; Pajaud, J.; Lepage, S.; Lucas-Clerc, C.; Bégué, J.-M.; Fromenty, B.; Robin, M.-A. Carbon tetrachloride-mediated lipid peroxidation induces early mitochondrial alterations in mouse liver. *Lab. Invest.* **2012**, *92*, 396-410,https://doi.org/10.1038/labinvest.2011.193.
40. Cho, K.-A.; Woo, S.-Y.; Seoh, J.-Y.; Han, H.-S.; Ryu, K.-H. Mesenchymal stem cells restore CCl4-induced liver injury by an antioxidative process. *Cell Biol. Int.* **2012**, *36*, 1267-1274,https://doi.org/10.1042/CBI20110634.
41. Heeba, G.H.; Morsy, M.A. Fucoidan ameliorates steatohepatitis and insulin resistance by suppressing oxidative stress and inflammatory cytokines in experimental non-alcoholic fatty liver disease. *Environ. Toxicol. Pharmacol.* **2015**, *40*, 907-914,https://doi.org/10.1016/j.etap.2015.10.003.
42. Heeba, G.H.; Mahmoud, M.E. Therapeutic potential of morin against liver fibrosis in rats: Modulation of oxidative stress, cytokine production and nuclear factor kappa B. *Environ. Toxicol. Pharmacol.* **2014**, *37*, 662-671, https://doi.org/10.1016/j.etap.2014.01.026.
43. Lijnen, P.; Petrov, V.; Rumilla, K.; Fagard, R. Transforming Growth Factor-β. *Methods Find. Exp. Clin. Pharmacol.* **2003**, *25*, 79-86,https://doi.org/10.1358/mf.2003.25.2.723680.
44. Wang, Y.-r.; Hong, R.-t.; Xie, Y.-y.; Xu, J.-m. Melatonin Ameliorates Liver Fibrosis Induced by Carbon Tetrachloride in Rats via Inhibiting TGF-β1/Smad Signaling Pathway. *Current Medical Science* **2018**, *38*, 236-244,https://doi.org/10.1007/s11596-018-1871-8.
45. Masszi, A.; Kapus, A. Smaddening complexity: the role of Smad3 in epithelial-myofibroblast transition. *Cells Tissues Organs* **2011**, *193*, 41-52,https://doi.org/10.1159/000320180.
46. Prestigiacomo, V.; Weston, A.; Messner, S.; Lampart, F.; Suter-Dick, L. Pro-fibrotic compounds induce stellate cell activation, ECM-remodelling and Nrf2 activation in a human 3D-multicellular model of liver fibrosis. *PLoS One* **2017**, *12*, e0179995,https://doi.org/10.1371/journal.pone.0179995.
47. Jiang, J.X.; Chen, X.; Serizawa, N.; Szyndralewiez, C.; Page, P.; Schröder, K.; Brandes, R.P.; Devaraj, S.; Török, N.J. Liver fibrosis and hepatocyte apoptosis are attenuated by GKT137831, a novel NOX4/NOX1 inhibitor in vivo. *Free Radical Biol. Med.* **2012**, *53*, 289-296, https://doi.org/10.1016/j.freeradbiomed.2012.05.007.
48. Khalil, M.R.; El-Demerdash, R.S.; Elminshawy, H.H.; Mehanna, E.T.; Mesbah, N.M.; Abo-Elmatty, D.M. Therapeutic effect of bone marrow mesenchymal stem cells in a rat model of carbon tetrachloride induced liver fibrosis. *Biomedical Journal* **2020**,https://doi.org/10.1016/j.bj.2020.04.011.
49. Alzahrani, F.A.; El-Magd, M.A.; Abdelfattah-Hassan, A.; Saleh, A.A.; Saadeldin, I.M.; El-Shetry, E.S.; Badawy, A.A.; Alkarim, S. Potential Effect of Exosomes Derived from Cancer Stem Cells and MSCs on Progression of DEN-Induced HCC in Rats. *Stem Cells Int.* **2018**, *2018*, 8058979,https://doi.org/10.1155/2018/8058979.
50. Li, L.; Zhang, S.; Zhang, Y.; Yu, B.; Xu, Y.; Guan, Z. Paracrine action mediate the antifibrotic effect of transplanted mesenchymal stem cells in a rat model of global heart failure. *Mol. Biol. Rep.* **2009**, *36*, 725-731,https://doi.org/10.1007/s11033-008-9235-2.
51. Wu, Y.; Huang, S.; Enhe, J.; Ma, K.; Yang, S.; Sun, T.; Fu, X. Bone marrow-derived mesenchymal stem cell attenuates skin fibrosis development in mice. *Int. Wound J.* **2014**, *11*, 701-710,https://doi.org/10.1111/iwj.12034.
52. Aithal, A.P.; Bairy, L.K.; Seetharam, R.N.; Kumar, N. Hepatoprotective effect of bone marrow-derived mesenchymal stromal cells in CCl4-induced liver cirrhosis. *3 Biotech* **2021**, *11*, 107,https://doi.org/10.1007/s13205-021-02640-y.
53. Milosavljevic, N.; Gazdic, M.; Simovic Markovic, B.; Arsenijevic, A.; Nurkovic, J.; Dolicanin, Z.; Jovicic, N.; Jeftic, I.; Djonov, V.; Arsenijevic, N.; Lukic, M.L.; Volarevic, V. Mesenchymal stem cells attenuate liver

fibrosis by suppressing Th17 cells – an experimental study. *Transplant Int.* **2018**, *31*, 102-115, https://doi.org/10.1111/tri.13023.
54. Baertschiger, R.M.; Serre-Beinier, V.; Morel, P.; Bosco, D.; Peyrou, M.; Clément, S.; Sgroi, A.; Kaelin, A.; Buhler, L.H.; Gonelle-Gispert, C. Fibrogenic Potential of Human Multipotent Mesenchymal Stromal Cells in Injured Liver. *PLoS One* **2009**, *4*, e6657,https://doi.org/10.1371/journal.pone.0006657.
55. Chen, S.; Xu, l.; Lin, N.; Pan, W.; Hu, K.; Xu, R. Activation of Notch1 signaling by marrow-derived mesenchymal stem cells through cell–cell contact inhibits proliferation of hepatic stellate cells. *Life Sci*. **2011**, *89*, 975-981, https://doi.org/10.1016/j.lfs.2011.10.012.
56. Jiang, T.; Liao, W.; Charcosset, C. Recent advances in encapsulation of curcumin in nanoemulsions: A review of encapsulation technologies, bioaccessibility and applications. *Food Res. Int.* **2020**, *132*, 109035,https://doi.org/10.1016/j.foodres.2020.109035.
57. Roopa, G.; Roopa, K.; Jayanthi, C.; Mukunthan, S.; Akshay, K.K.S.; Hanumanthachar, K.J.; Goli, D. Enhanced Water Dispersibility of Curcumin Encapsulated in Alginate-Polysorbate 80 Nano Particles and Bioavailability in Healthy Human Volunteers. *Pharmaceutical Nanotechnology* **2019**, *7*, 39-56, https://doi.org/10.2174/2211738507666190122121242.
58. Marslin, G.; Prakash, J.; Qi, S.; Franklin, G. Oral Delivery of Curcumin Polymeric Nanoparticles Ameliorates CCl4-Induced Subacute Hepatotoxicity in Wistar Rats. *Polymers* **2018**, *10*,https://doi.org/10.3390/polym10050541.
59. Sasaki, T.; Sato, Y.; Kumagai, T.; Yoshinari, K.; Nagata, K. Effect of health foods on cytochrome P450-mediated drug metabolism. *Journal of Pharmaceutical Health Care and Sciences* **2017**, *3*, 14, https://doi.org/10.1186/s40780-017-0083-x.
60. Lee, H.-Y.; Kim, S.-W.; Lee, G.-H.; Choi, M.-K.; Jung, H.-W.; Kim, Y.-J.; Kwon, H.-J.; Chae, H.-J. Turmeric extract and its active compound, curcumin, protect against chronic CCl4-induced liver damage by enhancing antioxidation. *BMC Complement. Altern. Med.* **2016**, *16*, 316,https://doi.org/10.1186/s12906-016-1307-6.
61. Kang, H.-C.; Nan, J.-X.; Park, P.-H.; Kim, J.-Y.; Lee, S.H.; Woo, S.W.; Zhao, Y.-Z.; Park, E.-J.; Sohn, D.H. Curcumin inhibits collagen synthesis and hepatic stellate cell activation in-vivo and in-vitro. *J. Pharm. Pharmacol.* **2002**, *54*, 119-126, https://doi.org/10.1211/0022357021771823.
62. Rahmaniah, R.; Louisa, M.; Kusumawardhani, B.W.; Soetikno, V. Nano-Curcumin Inhibits Hepatic Stellate Cells Proliferations Induced by Alcohol by Inhibiting TGF-&#946. *Advanced Science Letters* **2017**, *23*, 6899-6902,https://doi.org/10.1166/asl.2017.9428.
63. Duarte, S.; Baber, J.; Fujii, T.; Coito, A.J. Matrix metalloproteinases in liver injury, repair and fibrosis. *Matrix Biol.* **2015**, *44-46*, 147-156, https://doi.org/10.1016/j.matbio.2015.01.004.
64. Wang, L.T.; Zhang, B.; Jie, J.C. Effect of anti-fibrosis compound on collagen expression of hepatic cells in experimental liver fibrosis of rats. *World J. Gastroenterol.* **2000**, *6*, 877,https://doi.org/10.3748/wjg.v6.i6.877.
65. Supriono, S.; Bogi, P.; Muhammad, K. Effects of Curcumin Against Matrix Metalloproteinase-2 (MMP-2) and Tissue Inhibitor Metalloproteinase-2 (TIMP-2) Serum Level on Rat Model of Liver Fibrosis Resolution Process. *Indonesian Journal of Gastroenterology, Hepatology, and Digestive Endoscopy* **2018**, *19*, 10-15, https://doi.org/10.24871/191201810-15.
66. Yang, Z.; He, C.; He, J.; Chu, J.; Liu, H.; Deng, X. Curcumin-mediated bone marrow mesenchymal stem cell sheets create a favorable immune microenvironment for adult full-thickness cutaneous wound healing. *Stem Cell. Res. Ther.* **2018**, *9*, 21,https://doi.org/10.1186/s13287-018-0768-6.
67. Hameeda, P.; Katti, S.; Jammalamadugu, R.; Bhatt, K.; Peram, M.R.; Kumbar, V. Comparison of Effects of Curcumin and Nano-curcumin on the Survival of Human-Derived Mesenchymal Stem Cells: An Experimental Study. *Journal of Advanced Oral Research* **2020**, *11*, 148-155,https://doi.org/10.1177/2320206820949741.
68. Wang, X.; Zhang, Y.; Yang, Y.; Zhang, W.; Luo, L.; Han, F.; Guan, H.; Tao, K.; Hu, D. Curcumin pretreatment protects against hypoxia/reoxgenation injury via improvement of mitochondrial function, destabilization of HIF-1α and activation of Epac1-Akt pathway in rat bone marrow mesenchymal stem cells. *Biomed. Pharmacother.* **2019**, *109*, 1268-1275, https://doi.org/10.1016/j.biopha.2018.11.005.